



ORIGINAL ARTICLE

Chemical extraction of cellulose from Ligno-cellulosic *Astragalus armatus* pods: Characterization, and application to the biosorption of methylene blue



Obaid F. Aldosari ^{a,*}, Mahjoub Jabli ^{a,b,*}, Moataz H. Morad ^c

^a Department of Chemistry, College of Science, Majmaah University, Al-Majmaah 11952, Saudi Arabia

^b Textile Materials and Processes Research Unit, Tunisia National Engineering School of Monastir, University of Monastir, Tunisia

^c Chemistry Department, Faculty of Applied Sciences, Umm Al-Qura University, Makkah 21955, Saudi Arabia

Received 9 March 2023; accepted 16 May 2023

Available online 22 May 2023

KEYWORDS

Astragalus armatus;
Extracted cellulose;
Bleaching;
Biosorption;
Methylene blue

Abstract The most widely available substrate, cellulose biopolymer, was shown to be used for several interesting applications such as pharmaceutical, composites, water treatment, textiles, etc. In this study, cellulose was chemically extracted from abundant *Astragalus armatus* pods through alkali and bleaching processes. The untreated biomass and the extracted polymer were characterized using FT-IR, XRD, SEM, and TGA-DTA analyses. FT-IR spectrum of the extracted cellulose confirmed that lignin and hemicellulose constituents were removed during alkali and bleaching treatments. The crystallinity index calculated for the extracted cellulose and the untreated *Astragalus armatus* pods were 38.2% and 25%, respectively. These small values proved the existence of the amorphous constituents in the composition of *Astragalus armatus*. The high crystallinity index calculated for the extracted cellulose confirmed the elimination of the amorphous constituents present in the untreated biomaterial. The change in the thermal decomposition indicated that the extracted cellulose was more thermally stable than the untreated biomass. At optimum conditions (T = 20 °C, pH = 6, and t = 60 min), the adsorption quantities were 165 mg/g and 148 mg/g of untreated *Astragalus armatus* pods, and extracted cellulose, respectively. The adsorption mechanism was non spontaneous and the interaction between the studied biomaterials and methylene blue

* Corresponding authors.

E-mail addresses: o.aldosari@mu.edu.sa (O.F. Aldosari), m.jabli@mu.edu.sa (M. Jabli).

Peer review under responsibility of King Saud University.



Production and hosting by Elsevier

was exothermic. Overall, the adsorption results demonstrated that the untreated *Astragalus armatus* pods and the extracted cellulose were excellent candidates for color uptake from water.

© 2023 The Author(s). Published by Elsevier B.V. on behalf of King Saud University. This is an open access article under the CC BY-NC-ND license (<http://creativecommons.org/licenses/by-nc-nd/4.0/>).

1. Introduction

The use of biopolymeric materials for environmental applications constitutes a promising technology for researchers due to their possession of numerous advantages (Simona et al., 2020; Vijay and Stefan, 2016; Muxika et al., 2017). The chemical treatment of the agricultural substrates results in several forms of materials such as active chemicals, biofuels, biopolymers, biofuels, etc. Indeed, the majority of the biomass residues are composed essentially of cellulose and lignin and other non-cellulose constituents (Morán et al., 2008; Alemdar and Sain, 2008; Jonoobi et al., 2009; Saravanakumar et al., 2013; Reddy et al., 2014; Gao et al., 2020; Sebeia et al., 2019; Sebeia et al., 2019; Tka et al., 2018). Cellulose biopolymer has attracted a particular interest, because it is widely applied in papermaking, reinforcing elements, textiles, pharmaceutical, wastewater treatment, composites, etc. Cellulose is present in different parts of the plants such as fruits, pods, leaves, barks, stalks, roots, etc. Following the literature review, several plants were demonstrated to be as sources of cellulose including *sisal* (Morán et al., 2008); *wheat straw* (Alemdar and Sain, 2008); *kenaf* (Jonoobi et al., 2009); *Prosopis juliflora* (Saravanakumar et al., 2013); *Agave* (Reddy et al., 2014), *Calotropis gigantean* (Gao et al., 2020); *Aegagropila Linnaei* (Sebeia et al., 2019), *Nerium oleander* (Sebeia et al., 2019); *Pergularia tomentosa* (Sebeia et al., 2019); *Populus tremula* (Tka et al., 2018), etc.

The existence of reactive hydroxyl groups in the chemical structure of cellulose make the biopolymer an excellent candidate for the adsorption of various kinds of organic and inorganic pollutants including metals, synthetic dyes, pesticides, carbon dioxide, etc. (Dimitrios et al., 2021; Suhas and Gupta, 2016). However, depending on the type of the adsorbate, the adsorption features of cellulose could be improved following several chemical modifications (Ahmed et al., 2022; Nilanjali et al., 2020; Ali et al., 2020).

Belonging to the family of Leguminosae, *Astragalus armatus* is naturally growing in the North of Africa (Algeria, Tunisia, and Morocco) and in the Gulf countries (Saudi Arabia, Kuwait, Iraq, etc.). It generally grows in the desert area and it is adapted to the austere climatic conditions. Although this plant is spontaneous and abundant, however its exploration remains limited. For example, the study of Moussaoui et al. (Younes et al., 2011) reported the use of the roots of *Astragalus armatus* as raw material for pulp and papermaking application. They confirmed the suitability of making paper sheets with a weight equal to 60 g/m² with good physical characteristics. Boual et al. (Zakaria et al., 2015) had successfully extracted a pure bioactive galactomannan polysaccharide, a water-soluble fraction from *Astragalus armatus*. Labeled et al. (Amira et al., 2016) had isolated the secondary metabolites and determined the bioactivities of *Astragalus armatus* pods. Recently, Mahmoudi et al (Maher et al., 2021) had extracted a series of lipids, fatty acids, proteins, and bioactive compounds from the *seeds* of three *Astragalus* species. In summary, the objective of the previous works was focalized only on the chemical and pharmacological studies on the *Astragalus* species (Xiaoxia et al., 2014). To our best knowledge, no investigation reported on the extraction of cellulose from *Astragalus* or the use of these biomaterials for the removal of toxic pollutants.

In the current work, cellulose polymer was extracted from *Astragalus armatus* pods through alkali and bleaching processes. The untreated biomass and the extracted cellulose were analyzed using many techniques including FT-IR, XRD, SEM, and TGA-DTA. The adsorption mechanism was assessed using methylene blue as a model of cationic dyes under the variation of several experimental fac-

tors. In particular, the influence of initial pH, initial methylene blue concentration, time of reaction, and temperature on the change of the adsorbed quantity was discussed. The theoretical kinetics and isotherms equations were used to better understand the adsorption process.

2. Experimental

2.1. Materials and reagents

Astragalus armatus pods were manually harvested from the forest of Al-zulfi, Riyadh (Saudi Arabia) during the month of May 2022. The chemicals of pure quality such as sodium hydroxide (NaOH), hydrogen peroxide (30%), and glacial acetic acid (99.5%) were used during alkali and bleaching processes without any further purifications. Methylene blue was purchased from the company of Sigma Aldrich and used in this study as an adsorbate model. The aqueous solutions were prepared using distilled water.

2.2. Chemical extraction of cellulose from *Astragalus armatus* clusters

Cellulose was extracted from *Astragalus armatus* pods following the previous published experimental protocols (Gao et al., 2020; Sebeia et al., 2019) with some modifications. In a first step, the harvested biomass was exhaustively washed with distilled water in attempts to remove the impurities attached on the biomass surface. Indeed, this stage of washing aims to mainly detach the sand and the diverse vegetable crusts from the studied biomass. Then, the biomass was spread, at room temperature, on a laboratory bench for drying during a week. An electrical grinder was used to transform the dried biomass into fine particles. After, the powdered biomass was thermally treated in a solution of NaOH (5 wt%) under the following conditions: liquor ratio = 1:50, T = 80 °C, and time = 120 min. During this main stage of chemical treatment, wax and also an important bulk of lignin were supposed to be removed. The resulting alkali treated *Astragalus armatus* pods were further treated during 120 min in a solution containing a mixture of glacial acetic acid and hydrogen peroxide (v/v = 1:1) (liquor ratio = 1:50, T = 90 °C). This stage allows the removal of the residual lignin and gives a bleach substance (Fig. 1). Lastly, the resulting polymer was filtered and dried at 60 °C during 6 h.

2.3. Characterization instruments

The studied biomasses were analyzed using an apparatus InfraLum FT-08 equipped with ATR. FT-IR spectra were realized in 32 scans with a resolution of 4 cm⁻¹ in the range from 400 to 4000 cm⁻¹. A Scanning Electron Microscope (JEOL JSM-5400) was used to evaluate the morphological properties of the studied materials. Samples were covered with gold metal using a vacuum sputter-coater to enhance the con-

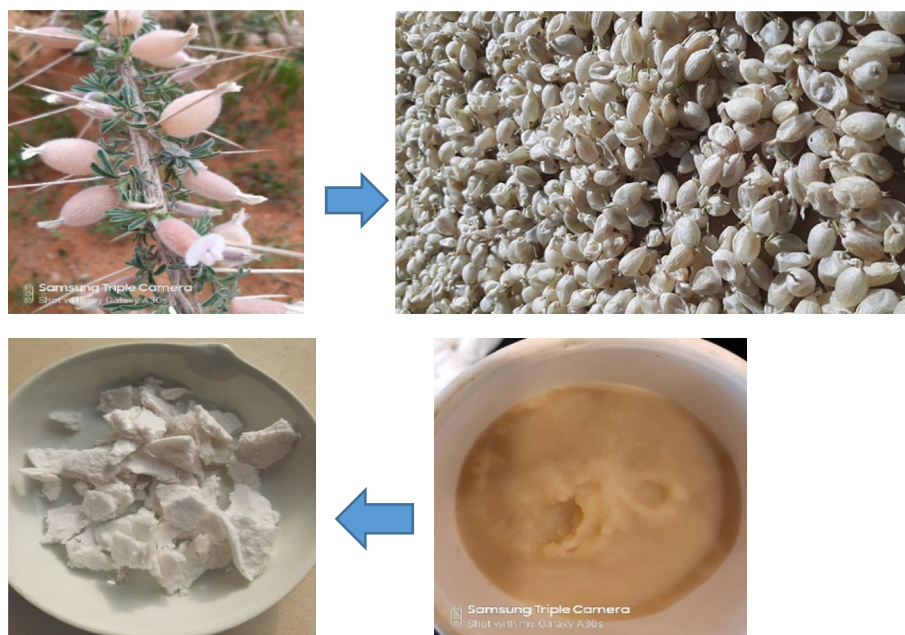


Fig. 1 Some photographs demonstrating the major steps used for the extraction of cellulose from *Astragalus armatus* pods.

ductivity and the quality of the samples image. The used accelerating voltage is equal to 20 kV. XRD patterns were obtained using PANalytical X'Pert PRO apparatus The 2 theta ranges from 10° to 90°. TGA/DTA curves were obtained using a platinum crucible with NETZSCH STA 449F3. The thermal analysis of untreated and treated *Astragalus armatus* pods was carried out in air flow at 10°/min a heating rate.

2.4. Bio sorption of methylene blue dye using untreated and treated *Astragalus armatus*

A batch mode system was implemented to evaluate the adsorption capacity of untreated and treated *Astragalus armatus* toward methylene blue. A mass of 0.01 g of the biomass was mixed with a volume of 20 mL of methylene blue in an Erlenmeyer flask and stirred at a constant agitation speed (150 rpm). After the required period of time, the mixture was filtered using a filter paper and the absorbance of the solution was determined at the maximum wavelength (666 nm). The biosorption experiments were carried out at different experimental conditions such as: initial pH change (3 to 10), time (0–120 min), initial dye concentration (0–1000 mg/L), and temperature (20–50 °C).

Equation (1) was used to calculate the adsorbed quantity, q (mg/g), of methylene blue onto the adsorbents surface:

$$q(\text{mg/g}) = \frac{(C_0 - C_e)}{m} \times V \quad (1)$$

C_0 and C_e are the concentrations of methylene blue dye at initial and equilibrium state, respectively. m and V are the mass of the adsorbent and the volume of the adsorbate used throughout the experiments.

3. Results and discussion

It is important to underline that throughout the alkali treatment of *Astragalus armatus* pods, wax and a significant bulk

of lignin were supposed to be eliminated during this main step of chemical handling. Then, the treatment of the alkali biomass with CH_3COOH and H_2O_2 allows the complete removal of the residual lignin and offer a pure cellulosic substance. To interpret and confirm the chemical composition, the morphological, and the thermal characteristics of the untreated *Astragalus armatus* and the extracted cellulose, the materials were examined using FT-IR, XRD, SEM, and TGA-DTA.

3.1. FT-IR spectroscopy characterization

FT-IR spectroscopy analysis of untreated *Astragalus armatus* pods and extracted cellulose is given in Fig. 2. As it is observed, the studied biomaterials reveal similar absorption peaks which indicate the presence of the same main chemical groups (OH, CH, CH_2 , and C-O). However, the FT-IR spectrum of cellulose extracted from *Astragalus armatus* proves

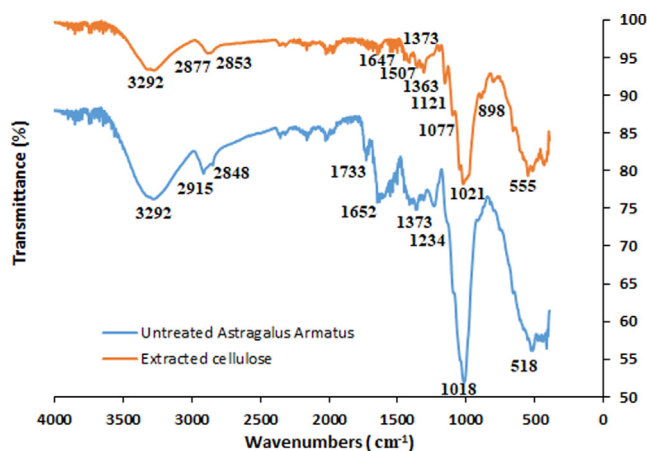


Fig. 2 FT-IR spectrum of untreated *Astragalus armatus* pods and extracted cellulose.

that lignin and hemicellulose were removed during alkali and bleaching processes. Indeed, the absorption peak observed at 1733 cm^{-1} for untreated *Astragalus armatus*, which corresponds to $\text{C}=\text{O}$ vibration of lignin and hemicellulose constituents (Gao et al., 2020; Sebeia et al., 2019), totally disappears in the spectrum of the resulting cellulose. The absorption peak observed at around 3292 cm^{-1} confirms the presence of hydroxyl groups for the biomass (Gao et al., 2020; Sebeia et al., 2019). Both $\text{C}-\text{H}$ stretching of $-\text{CH}_3$, and $-\text{CH}_2$ groups are seen in the range 2848 cm^{-1} and 2915 cm^{-1} (Gao et al., 2020; Sebeia et al., 2019). The peak observed at 1373 cm^{-1} is assigned to the angular deformation of $-\text{CH}$ groups. The peak at 1021 cm^{-1} is attributed to $\text{C}-\text{O}$ symmetric or asymmetric stretching vibration ($-\text{C}-\text{O}-\text{C}-$ ring) of cellulose. The peak at 898 cm^{-1} has been identified to be the out-of-plane angular deformation of the $-\text{CH}$ group (Gao et al., 2020; Sebeia et al., 2019).

3.2. Morphological analysis

Fig. 3 shows the morphological characteristics of untreated *Astragalus armatus* pods and extracted cellulose observed at different magnifications ($\times 200$ and $\times 1000$). The untreated biomass exhibits particles with irregular shapes with the presence of some impurities (Fig. 3a). However, after alkali and bleaching processes (Fig. 3b), the extracted cellulose appears more clean and condensed. This proves that the non-

cellulose constituents and some surface attached impurities have been totally removed.

3.3. XRD patterns

Fig. 4 shows the XRD patterns of the untreated *Astragalus armatus* pods and extracted cellulose. As it is observed from the resulting spectrum, the crystalline peaks showed no doublet in the intensity which proves that the studied biomasses are cellulose I (Maaloul et al., 2017; Zhang et al., 2018). The spectrum of the extracted cellulose displays three peaks located at 16° , 23° and 34.8° . According to literature, these observed peaks are assigned to (110), (200) and (040) lattice planes of the crystalline cellulose I (Zhang et al., 2018). However, the untreated *Astragalus armatus* pods showed the existence of peaks at 15.8° , 21° , 26° , and 28.5° . This indicates that the biomass contains also non-cellulose constituents including lignin, and hemicellulose.

Equation (2) was used to calculate the crystallinity index (CrI) of the studied biomaterials:

$$CrI(\%) = \frac{I_{200} - I_{am}}{I_{200}} \times 100 \quad (2)$$

I_{200} is the intensity of the maximum crystalline peak and I_{am} is the intensity of the principally amorphous peak.

The results indicated that the values of the crystallinity index calculated for the extracted cellulose and the untreated

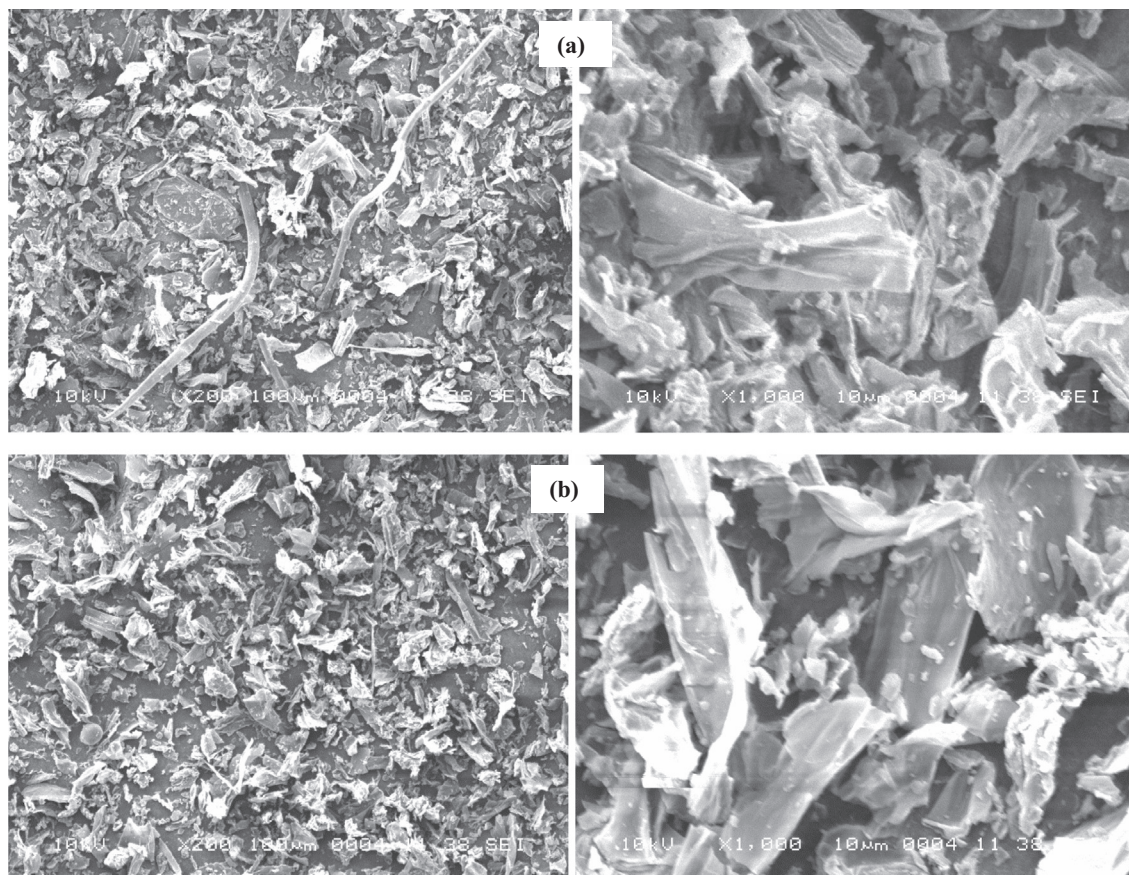


Fig. 3 SEM images, taken at different magnifications, of: (a) untreated *Astragalus armatus* and (b) extracted cellulose ($\times 200$ and $\times 1000$).

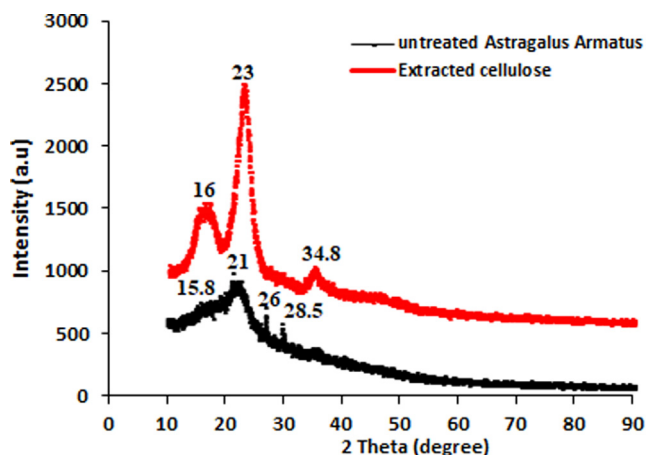


Fig. 4 XRD analysis of untreated *Astragalus armatus* pods and extracted cellulose.

Astragalus armatus pods are equal to 38.2% and 25%, respectively. These values, which are relatively small, prove the existence of amorphous compounds in the composition of *Astragalus armatus* such as lignin and hemicelluloses (Reddy et al., 2014; Millogo et al., 2020). Compared to the untreated biomass, the high crystallinity index calculated for the extracted cellulose confirms again the elimination of the amorphous constituents present in the virgin biomaterial (Reddy et al., 2014; Millogo et al., 2020). These results agree also with FT-IR data.

3.4. Thermal examination

The thermal stability of untreated *Astragalus armatus* pods and extracted cellulose are assessed through TGA/DTA analysis as shown in Fig. 5. The thermal decomposition of untreated *Astragalus armatus* occurs into different pyrolysis steps due to several reaction stages. In details, at low temperature values, the studied biomaterials display slight weight losses. As it is observed, the untreated biomass exhibits a first mass loss of 6% at 73 °C. Whereas, at approximately the same temperature (72 °C), the weight loss for the extracted cellulose is about 3%. This difference in weight loss between the two biomaterials proves that the untreated biomass contains more hydrophilic substrates compared to the extracted polymer. It is well recognized that the weight loss observed during this first stage is assigned to the evaporation of adsorbed water molecules and moisture contained in the natural products (Ramesh et al., 2020). At high temperature values, the maximum weight loss achieves 92% and 96% for untreated *Astragalus armatus* and extracted cellulose, respectively. The DTA curve of the untreated *Astragalus armatus* pods (Fig. 5a) demonstrates two exothermic peaks observed at 318 °C and 462 °C which could possibly be related to the main pyrolytic reaction of cellulose polymer and the oxidation of the charred residues. However, the DTA curve of the extracted polymer (Fig. 5b) displays only one exothermic peak observed at a higher temperature (351 °C). This significant variation in thermal decomposition indicates that the extracted cellulose is more thermally stable than the untreated biomass. Such variation in thermal result confirms again the chemical modification of *Astragalus armatus* clusters.

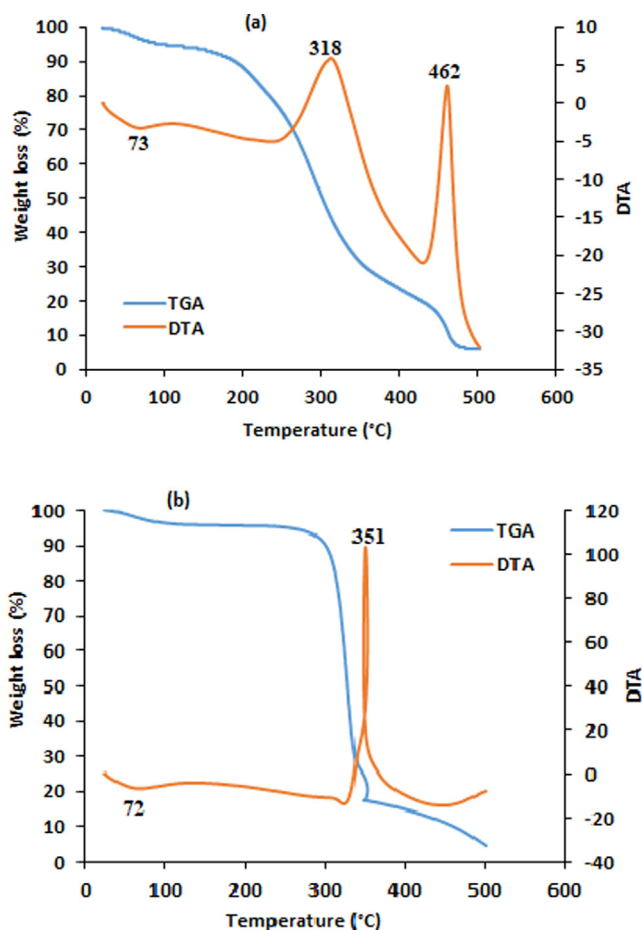


Fig. 5 TGA/DTA curves of untreated *Astragalus armatus* pods and extracted cellulose.

3.5. Application of untreated *Astragalus armatus* pods and extracted cellulose to the adsorption of methylene blue

3.5.1. Influence of experimental factors change on adsorption

Fig. 6a elucidates the evolution of the adsorbed quantity of methylene blue on the surface of the studied biomaterials versus the initial pH variation ($C_0 = 30$ mg/L, time = 60 min, $T = 20$ °C). As it is displayed, the highest adsorption capacity was revealed when the initial pH value is equal to 6. The obtained experimental curves show also different trends with relation to the variation of the adsorption capacity of methylene blue against pH. It is supposed that when the solution is more acidic, more protons H^+ are available which cause the electrostatic repulsion between the cationic charges of methylene blue and the protons. However, when the solution becomes alkaline, the forces of attraction between the positive charges of the cationic dye and the negative hydroxyl groups of the cellulosic substrates are more important and consequently the adsorption capacity is more significant.

Fig. 6b, c highlight the variation of the adsorbed quantity of methylene blue as a function of reaction time (pH = 6, $T = 20$ °C). From the plots, results indicate that the adsorption rate, using the studied biomaterials, is very fast and only a period of 20 min of reaction is necessary to achieve the adsorption equilibrium. It is also important to note that the

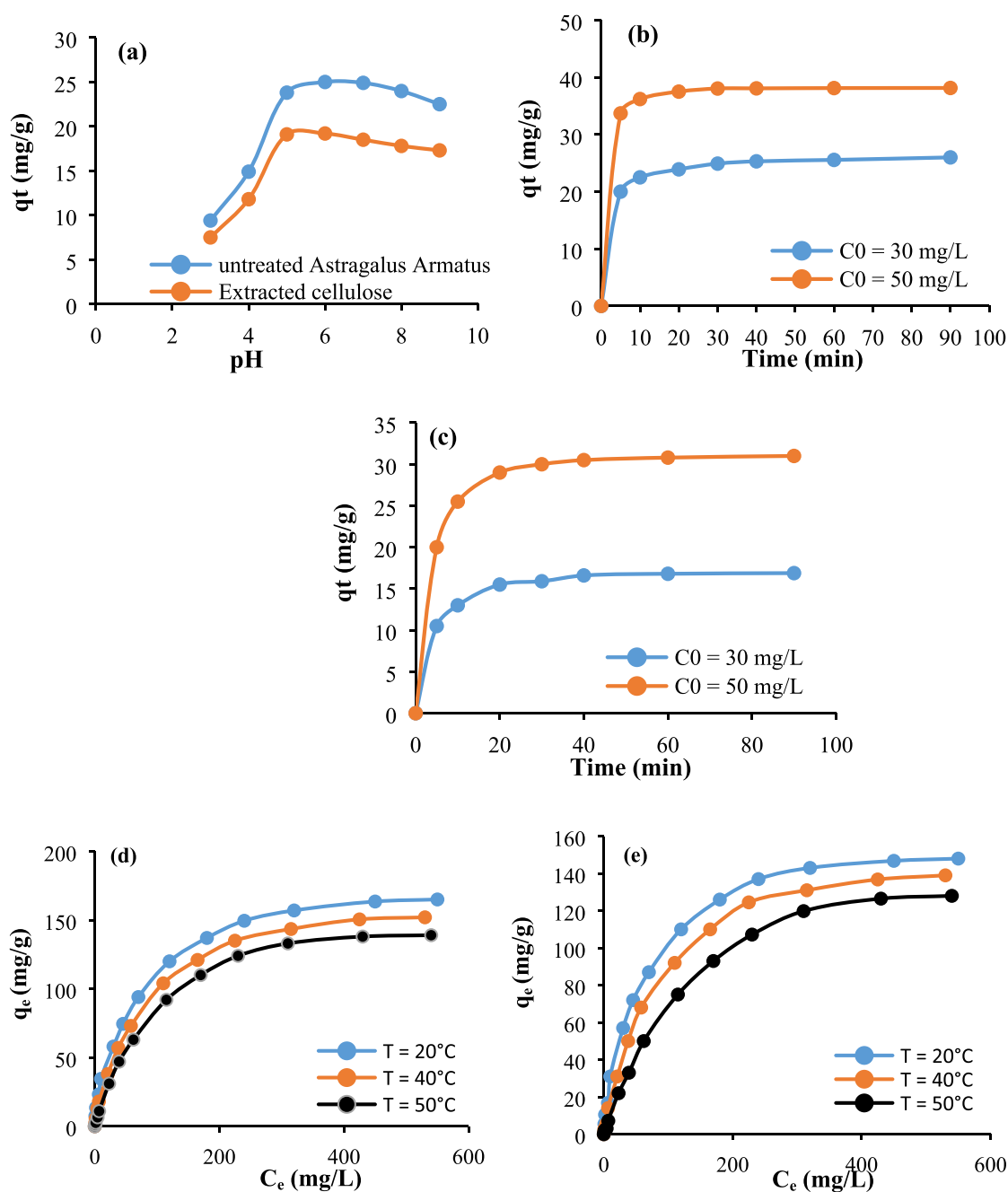


Fig. 6 Progress of the adsorbed quantity of methylene blue as a function of: (a) pH, (b) time, (untreated *Astragalus armatus*), (c) time (extracted cellulose), (d) isotherms (untreated *Astragalus armatus*), and (e) isotherms (extracted cellulose).

obtained curves display two main phases distinguishing the adsorption kinetic profile. During the initial few minutes (05 min), the adsorption rate of methylene blue proceeds promptly and approximately 90 to 95% of the target is realized. This trend is justified by the accessibility of voluminous adsorption sites at the surface of the biomaterials at this first stage of reaction. However, when the reaction exceeds a period of 10 min, the adsorption becomes slow and it achieves the maximum level at about 20 min. This constitutes a proof of the saturation of the adsorption sites at this final adsorption phase.

The influence of the change in temperature and methylene blue concentration (pH = 6, Time = 60 min) on the adsorption capacity is elucidated in Fig. 6d, e. Results demonstrate that the untreated *Astragalus armatus* pods and extracted cellulose are good adsorbents of methylene blue. Indeed, at optimum conditions ($T = 20^\circ\text{C}$, pH = 6, and $t = 60$ min), the adsorption quantities are found to be 165 mg/g and 148 mg/g of for untreated *Astragalus armatus* pods and extracted cellulose, respectively. The slight difference observed in the adsorbed quantity of methylene blue between the two studied biomaterials is justified by the elimination of the non-cellulose

constituents during the alkali and bleaching processes. As it is also shown, the adsorption capacity depends on the temperature value and it decreases with the increase of temperature. This exothermic effect may be due to the reduction of the interaction between methylene blue and the reactive sites of the biomaterials. For instance, in the case of the untreated *Astragalus armatus*, the maximum adsorption quantity decreases from 165 mg/g to 139 mg/g when the temperature is increased from 20 °C to 50 °C. It is worth to mention that the capacity of the adsorption of methylene blue using the biomaterials studied in this work is in some cases much higher than other published biomaterials and in other cases comparable (Kumar and Kumaran, 2005; Vadivelan and Kumar, 2005; Annadurai et al., 2002; Banerjee and Dastidar, 2005; Sajab et al., 2011; Nasuha et al., 2010; Belala et al., 2011).

3.5.2. Kinetic study

The kinetic equations of pseudo first order (Fig. 7a and Fig. 8a), pseudo second order (Fig. 7b and Fig. 8b), Elovich (Fig. 7c and Fig. 8c), and intra-particle diffusion (Fig. 7d and Fig. 8d) are used in their linearized forms to better consider the adsorption process of methylene blue in the presence of *Astragalus armatus* and extracted cellulose. The theoretical parameters and the regression coefficients are computed and elucidated in Tables 1 and 2. As it is clearly shown in the provided results, for the pseudo second order plots, the calculated theoretical adsorption quantities are found to be close to the

values measured experimentally and also the regression coefficients are close to 0.99. This result acclaims that the adsorption process can be considered as chemical and therefore the studied biomaterials and methylene blue molecules can interact through electrostatic or strong interactions (Kumar and Kumaran, 2005; Nasuha et al., 2010). As it is also revealed from the resulting curves, The Intra-particle diffusion plots (Fig. 7d and Fig. 8d) deviate from the origin which may demonstrate that the adsorption mechanism assessed using the studied biomaterials is characterized by not only an intra-particle diffusion but also other kinetic processes can take place (Kumar and Kumaran, 2005; Nasuha et al., 2010).

3.5.3. Thermodynamic study of the adsorption mechanism

The linearized isotherms equations of Langmuir (Fig. 9a and Fig. 10a), Freundlich (Fig. 9b and Fig. 10b), and Temkin (Fig. 9c and Fig. 10c) are used to better understand the interaction between methylene blue, *Astragalus armatus*, and extracted cellulose. The calculated isotherms constants, and the regression coefficients are given in Tables 1 and 2. As it is shown from the results, the regression coefficients are close to 0.99 in the case of Langmuir isotherm. This tendency clarifies that the reactive adsorption sites are distributed homogeneously on the surface of *Astragalus armatus* and the extracted cellulose. Indeed, the straight lines (Fig. 9a and Fig. 10a) prove the formation of the monolayers (Guo et al., 2014). Regarding, the Freundlich results, the obtained regression coefficients are

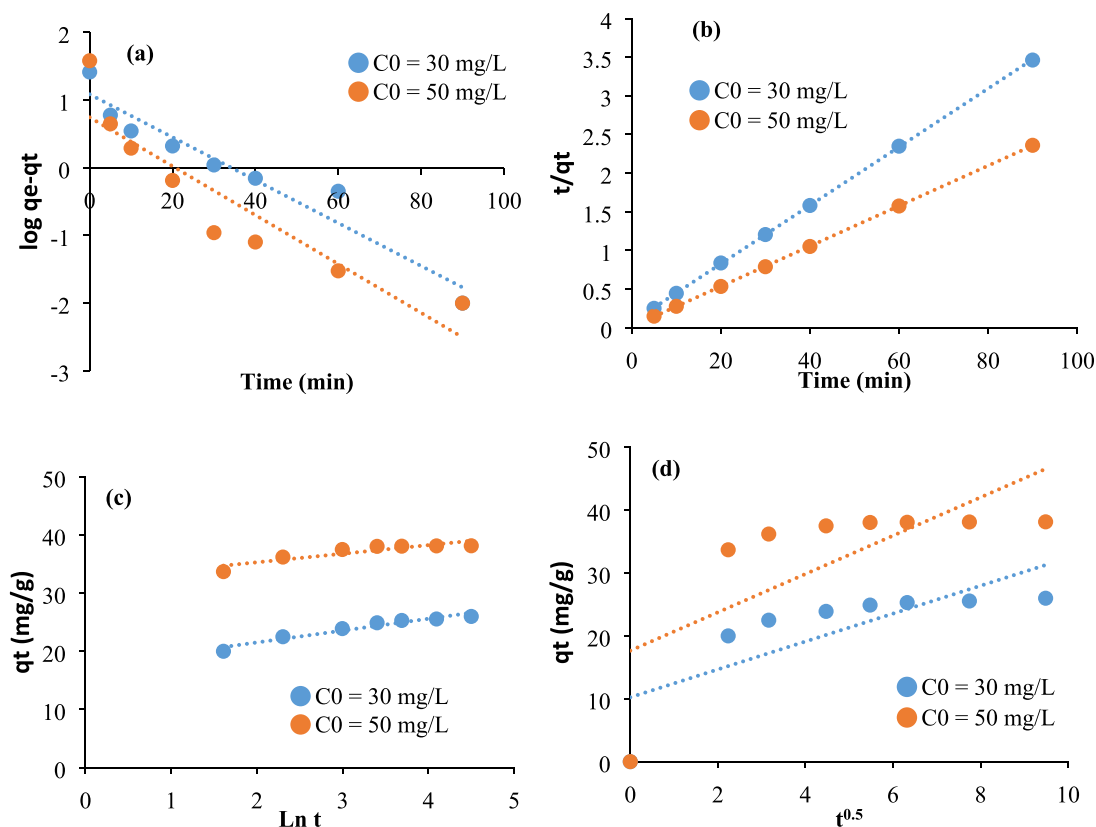


Fig. 7 Linearization of the experimental kinetic data related to untreated *Astragalus armatus* through the equations of: (a) First pseudo order, (b) Pseudo second order, (c), and (d) Intra-particle diffusion.

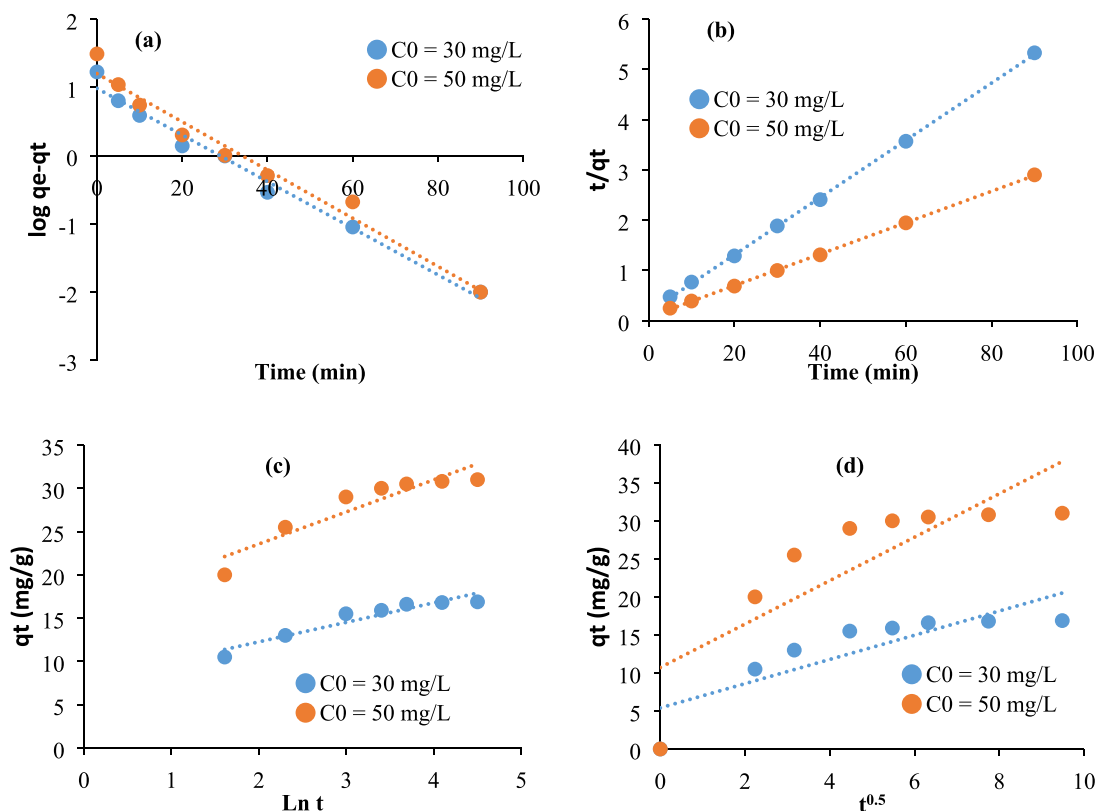


Fig. 8 Linearization of the experimental kinetic data related to extracted cellulose through the equations of: (a) First pseudo order, (b) Pseudo second order, (c), and (d) Intra-particle diffusion.

Table 1 Calculated kinetic data, isotherms constants, and regression coefficients related to the adsorption of methylene blue on the surface of the untreated *Astragalus armatus*.

Kinetic equations	Constants	Dye concentration (mg/L)		Isotherms	Parameters	Temperature (°C)		
Pseudo first order	K_1 (min^{-1})	30	50	Langmuir	q_m ($\text{mg}\cdot\text{g}^{-1}$)	20	40	50
	q ($\text{mg}\cdot\text{g}^{-1}$)	0.032	0.036		K_L ($\text{L}\cdot\text{g}^{-1}$)	178.57	169.49	163.93
	R^2	12.16	17.52		R^2	0.021	0.016	0.01
Pseudo second order	K_2	0.93	0.84	Thermodynamic parameters	ΔH° (KJ mol^{-1})	0.99	0.99	0.99
	q	0.011	0.006		ΔS° (J mol^{-1})	-3.35		
	R^2	26.46	38.46		ΔG° (KJ mol^{-1})	2.47	2.87	3.07
Elovich	α ($\text{mg}\cdot\text{g}^{-1}\cdot\text{min}^{-1}$)	1.06 $\times 10^4$	4.8 $\times 10^9$	Freundlich	K_F ($\text{L}\cdot\text{g}^{-1}$)	186.2	36.81	6.19
	β ($\text{mg}\cdot\text{g}^{-1}\cdot\text{min}^{-1}$)	0.49	0.68		n	2.02	1.62	1.36
	R^2	0.94	0.81		R^2	0.97	0.96	0.96
Intra-particle-Diffusion	K ($\text{mg}\cdot\text{g}^{-1}\cdot\text{min}^{1/2}$)	2.22	3.05	Temkin	b_T (J $\cdot\text{mol}^{-1}$)	86.11	100.82	110.74
	R^2	0.6	0.5		A ($\text{L}\cdot\text{g}^{-1}$)	1.81	1.87	2.31
					R^2	0.94	0.93	0.91

also high and they range from 0.96 to 0.97. This clarifies that the adsorption mechanism is too complex to conclude on its mode. The parameter n of the Freundlich model ranges from

1.33 to 2.02 which may suppose that the biosorption of methylene blue using *Astragalus armatus* and the extracted cellulose is favorable at the current conditions (Treybal, 1981).

Table 2 Calculated kinetic data, isotherms constants, and regression coefficients related to the adsorption of methylene blue on the surface of the extracted cellulose.

Kinetic equations	Constants	Dye concentration (mg/L)		Isotherms	Parameters	Temperature (°C)		
Pseudo first order	K_1 (min^{-1})	30	50	Langmuir	q_m ($\text{mg}\cdot\text{g}^{-1}$)	20	40	50
	q ($\text{mg}\cdot\text{g}^{-1}$)	0.034	0.035		K_L ($\text{L}\cdot\text{g}^{-1}$)	161.29	154.5	149.8
	R^2	9.68	15.85		R^2	0.021	0.013	0.007
Pseudo second order	K_2	0.98	0.97	Thermodynamic parameters	ΔH° (KJ mol^{-1})	0.99	0.99	0.99
	q	0.0011	0.0003		ΔS° (J mol^{-1})	-2.65		
	R^2	17.54	32.25		ΔG° (KJ mol^{-1})	2.74	3.1	3.29
Elovich	α ($\text{mg}\cdot\text{g}^{-1}\cdot\text{min}^{-1}$)	102.33	13.8	Freundlich	K_F ($\text{L}\cdot\text{g}^{-1}$)	1.9	1.49	1.33
	β ($\text{mg}\cdot\text{g}^{-1}\cdot\text{min}^{-1}$)	0.96	0.96		n	0.96	0.96	0.97
	R^2	0.9	0.86		b_T ($\text{J}\cdot\text{mol}^{-1}$)	93.96	108.47	123.18
Intra-particle-Diffusion	K ($\text{mg}\cdot\text{g}^{-1}\cdot\text{min}^{1/2}$)	1.86	2.09	Temkin	A ($\text{L}\cdot\text{g}^{-1}$)	1.86	2.09	2.65
	R^2	0.72	0.68		R^2	0.95	0.92	0.87

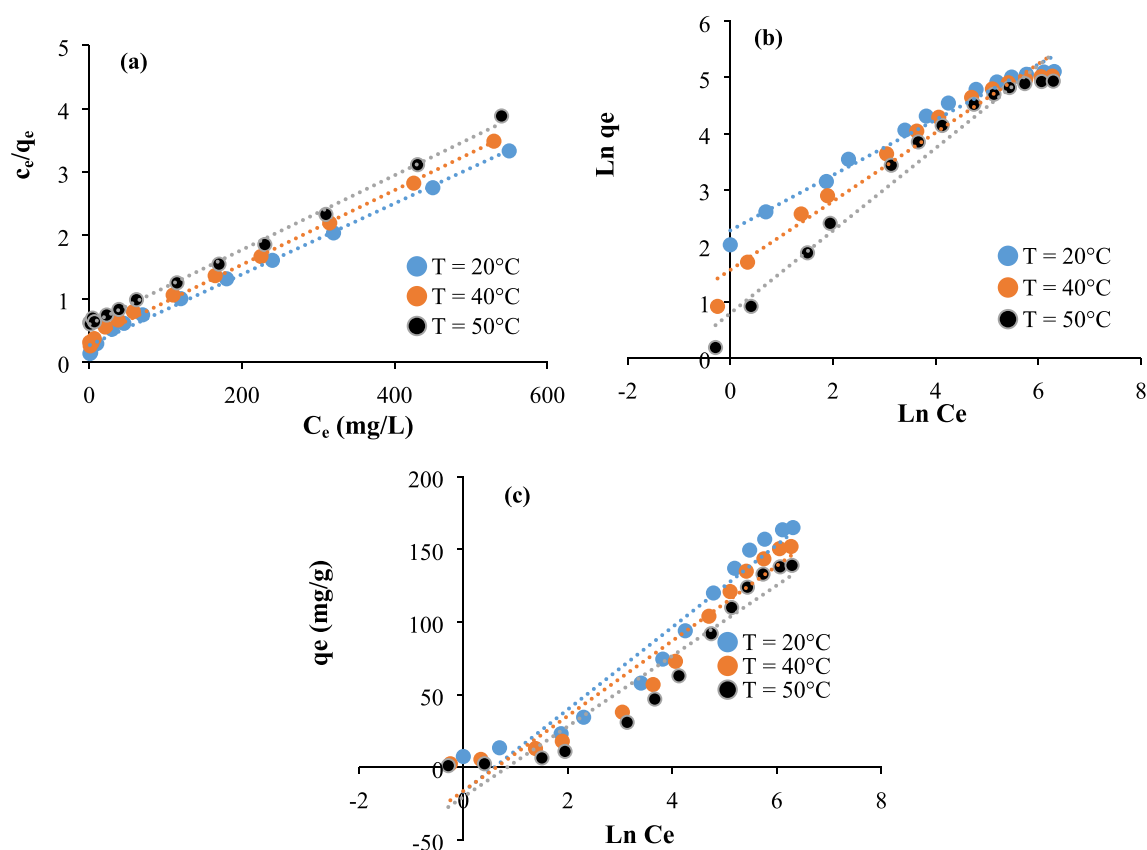

Fig. 9 Isotherms plots related to the untreated *Astragalus armatus*: (a) Langmuir, (b) Freundlich, and (c) Temkin.

Fig. 11 shows the plots of Logarithm K_d constants versus the inverse of temperature values related to the adsorption of methylene blue using *Astragalus armatus* and the extracted cellulose. The plots are used to calculate the enthalpy (ΔH°) and the entropy ΔS° parameters. The ΔH° values range from -2.65 to -2.35 KJ/mol. The small negative values of the enthalpy approve that the interaction between the studied biomaterials and methylene blue is exothermic. This result agrees with the decrease of the adsorbed quantiles of methy-

lene blue onto the biomaterials with the increase in temperature. The ΔS° values vary from -20 to -18.38 j/mol. The negative values of the entropy parameter indicate that the disorder decreases during the adsorption and some structural changes can take place (Omer et al., 2018). The ΔH° values are found to be in the range 2.47 to 3.29 KJ/mol. The positive sign of ΔG° parameter reveal that the adsorption of methylene blue is non spontaneous under the current experimental conditions.

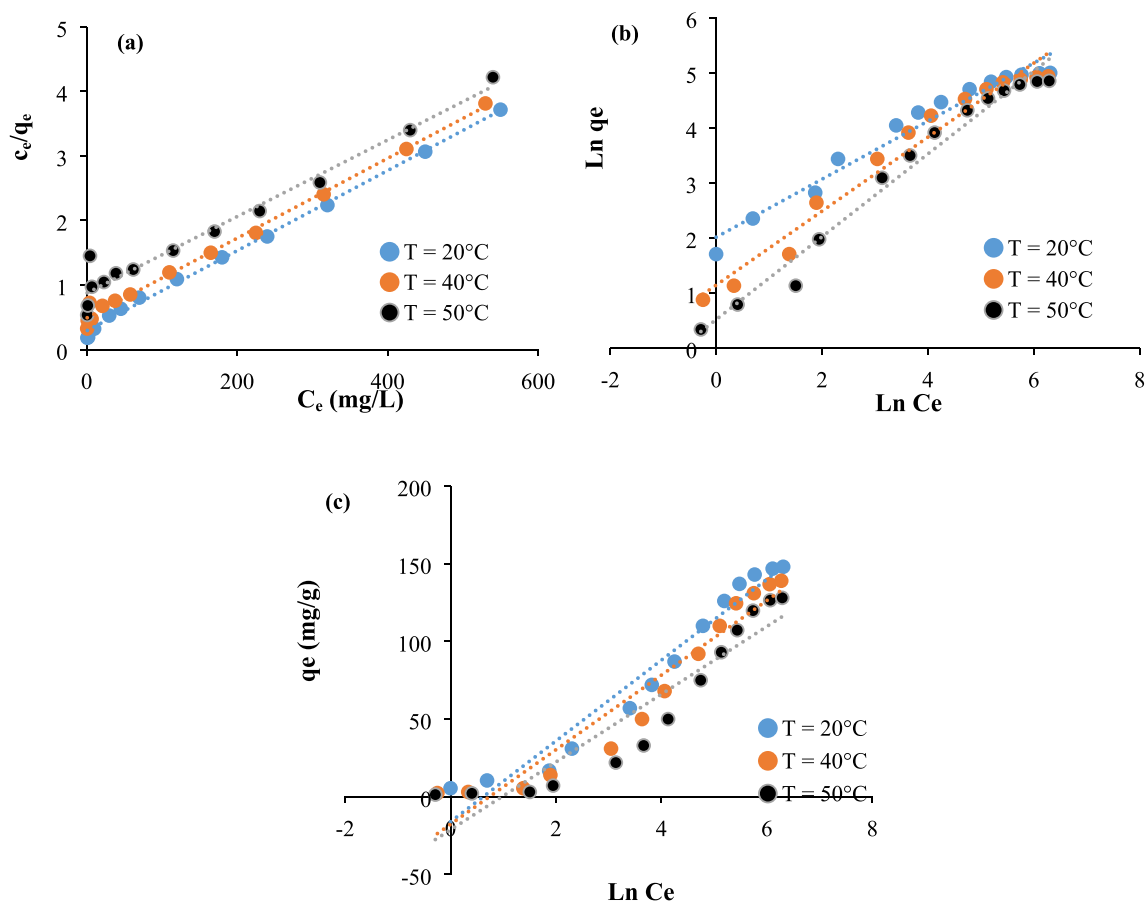


Fig. 10 Isotherms plots related to the extracted cellulose: (a) Langmuir, (b) Freundlich, and (c) Temkin.

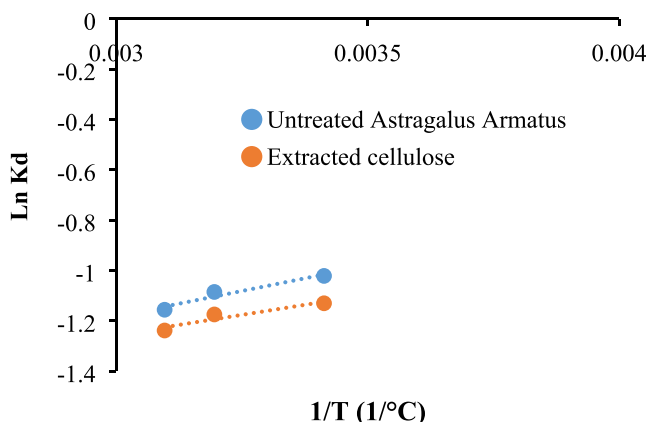


Fig. 11 Plots of Ln Kd versus $1/T$ related to the adsorption of methylene blue using *Astragalus armatus* and the extracted cellulose.

4. Conclusion

In this work, *Astragalus armatus* pods and the extracted cellulose were studied and used as adsorbents of methylene blue. The identification of the functional groups and the evidence of the removal of non-cellulosic constituents after chemical treatment was proved through FT-IR, XRD, SEM, and TGA-DTA analyses. The FT-IR of cellulose extracted from *Astragalus armatus* proved that lignin and hemicellulose were removed during the treatment of the biomass using alkali

and bleaching processes. SEM features indicated that the extracted cellulose was more clean and condensed suggesting that the non-cellulose constituents had been removed. The crystallinity index calculated for the extracted cellulose and the untreated *Astragalus armatus* pods were equal to 38.2% and 25%, respectively. The small values proved the existence of amorphous compounds in the composition of *Astragalus armatus* such as lignin and hemicelluloses. Compared to the untreated biomass, the high crystallinity index calculated for the extracted cellulose confirmed again the elimination of the amorphous constituents present in the virgin biomaterial. The DTA curve of the untreated *Astragalus armatus* pods demonstrated two exothermic peaks at 318 °C and 462 °C. However, the DTA curve of the extracted polymer displayed only one exothermic peak at 351 °C. The change in thermal property indicated that the extracted cellulose was more thermally stable than the untreated biomass. The adsorption results demonstrated that the untreated *Astragalus Armatus* pods and extracted cellulose were good adsorbents of methylene blue. At optimum conditions, the adsorption quantities were 165 mg/g and 148 mg/g for untreated biomass, and extracted cellulose, respectively. The adsorption was non spontaneous and exothermic. Further experiments will be extended to conduct chemical modifications on the extracted cellulose using amine reagents and check the aptitude of the resulting materials to remove other toxic pollutants.

Declaration of Competing Interest

The authors declare that they have no known competing financial interests or personal relationships that could have appeared to influence the work reported in this paper.

Acknowledgments

The authors would like to thank Deanship of Scientific Research at Majmaah University for supporting this work under Project No. R-2023-440.

References

- Ahmed, I.W., Maaly, A.K., Hanaa, M.A., Islam, M.A., 2022. Application of amino-functionalized cellulose-poly(glycidyl methacrylate) graft copolymer (AM-Cell-g-PGMA) adsorbent for dyes removal from wastewater. *Clean. Eng. Technol.* 6, 100374.
- Alemdar, A., Sain, M., 2008. Isolation and characterization of nanofibers from agricultural residues Wheat straw and soy hulls. *Bioresour. Technol.* 99 (6), 1664–1671.
- Ali, H.J., Ahmed, S.A., Mohd, S.M., 2020. Acid-fractionalized biomass material for methylene blue dye removal: a comprehensive adsorption and mechanism study. *J. Taibah Univ. Sci.* 14 (1), 305–313.
- Amira, L., Maria, F., Ilhem, L.-Z., Erhan, K., Sakina, Z., Laurence, V.-N., Abdulmagid, A.M., Zahia, S., Ahmed, K., Zahia, K., Mehmet, Ö., 2016. Compounds from the pods of *Astragalus armatus* with antioxidant, anticholinesterase, antibacterial and phagocytic activities. *Pharm. Biol.* 54, 3026–3032.
- Annadurai, G., Juang, R.-S., Lee, D.-J., 2002. Use of cellulose-based wastes for adsorption of dyes from aqueous solutions. *J. Hazard. Mater.* 92, 263–274.
- Banerjee, S., Dastidar, M.G., 2005. Use of jute processing wastes for treatment of wastewater contaminated with dye and other organics. *Bioresour. Technol.* 96, 1919–1928.
- Belala, Z., Jeguirim, M., Belhachemi, M., Addoun, F., Trouve, G., 2011. Biosorption of basic dye from aqueous solutions by date palm trees: Kinetic, equilibrium and thermodynamic studies. *Desalination* 271, 80–87.
- Dimitrios, G., Abdelhamid, H.N., Li, J., Ulrica Edlund, Aji, P., 2021. Mathew. All-cellulose functional membranes for water treatment: Adsorption of metal ions and catalytic decolorization of dyes. *Carbohydrate Polymers* 264, 118044.
- Gao, A., Chen, H., Tang, J., Xie, K., Hou, A., 2020. Efficient extraction of cellulose nanocrystals from waste *Calotropis gigantea* fiber by SO₄²⁻/TiO₂ nano-solid superacid catalyst combined with ball milling Exfoliation. *Ind. Crop. Prod.* 152, 112524.
- Guo, J.-Z., Li, B., Liu, L., Lv, K., 2014. Removal of methylene blue from aqueous solutions by chemically modified bamboo. *Chemosphere* 111, 225–231.
- Jonoobi, M., Harun, J., Mishra, M., Oksman, K., 2009. Chemical composition, crystallinity and thermal degradation of bleached and unbleached kenaf bast (*Hibiscus cannabinus*) pulp and nanofiber. *BioResources* 4 (2), 626–639.
- Kumar, K.V., Kumaran, A., 2005. Removal of methylene blue by mango seed kernel powder. *Biochem. Eng. J.* 27, 83–93.
- Maaloul, N., Ben Arfi, R., Rendueles, M., Ghorbal, A.M., Diaz, M., 2017. Dialysis-free extraction and characterization of cellulose crystals from almond (*Prunus dulcis*) shells. *J. Mater. Environ. Sci.* 8, 4171–4181.
- Maher, M., Raoudha, A., Fayçal, B., Boutheina, Y., Mahmoud, M., Nizar, N., 2021. Characterization of lipids, proteins, and bioactive compounds in the seeds of three *Astragalus* species. *Food Chem.* 339, 127824.
- Millogo, Y., Aubert, J.-E., Hamard, E., Morel, J.-C., 2020. How properties of Kenaf fibers from Burkina Faso contribute to the reinforcement of earth blocks. *Materials* 8, 2332–2345.
- Morán, J.I., Alvarez, V.A., Cyras, V.P., Vázquez, A., 2008. Extraction of cellulose and preparation of nanocellulose from sisal fibers. *Cellul.* 15, 149.
- Muxika, A., Etxabide, A., Uranga, J., Guerrero, P., de la Caba, K., 2017. Chitosan as a bioactive polymer: processing, properties and applications. *Int. J. Biol. Macromol.* 105 (part 2), 1358–1368.
- Nasuha, N., Hameed, B.H., Din, A.T., 2010. Rejected tea as a potential low-cost adsorbent for the removal of methylene blue. *J. Hazard. Mater.* 175, 126–132.
- Nilanjali, M., Swarnima, R., Narender, K.G., Shubhangi, A.S., Virendra, K., 2020. Radiation grafted cellulose fabric as reusable anionic adsorbent: a novel strategy for potential large-scale dye wastewater remediation. *Carbohydr. Polym.* 249, 116902.
- Omer, O.S., Hussein, M.A., Hussein, B.H.M., Mgaidi, A., 2018. Adsorption thermodynamics of cationic dyes (methylene blue and crystal violet) to a natural clay mineral from aqueous solution between 293.15 and 323.15 K. *Arab. J. Chem.* 11, 615–623.
- Ramesh, G.K., Subramanian, S., Sathiyamurthy, S., Prakash, M., 2020. *Calotropis Gigantea* fiber-epoxy composites: Influence of fiber orientation on mechanical properties and thermal behavior. *J. Nat. Fibers* 19 (3), 1–13.
- Reddy, K.O., Zhang, J., Zhang, J., Rajulu, A.V., 2014. Preparation and properties of self-reinforced cellulose composite films from *Agave microfibrils* using an ionic liquid. *Carbohydr. Polym.* 114, 537–545.
- Sajab, M.S., Chia, C.H., Zakaria, S., Jani, S.M., Ayob, M.K., Chee, K.L., Khiew, P.S., Chiu, W.S., 2011. Citric acid modified kenaf core fibres for removal of methylene blue from aqueous solution. *Bioresour. Technol.* 102, 7237–7243.
- Saravanakumar, S.S., Kumaravel, A., Nagarajan, T., Sudhakar, P., Baskaran, R., 2013. Characterization of a novel natural cellulosic fiber from *Prosopis juliflora* bark. *Carbohydr. Polym.* 92 (2), 1928–1933.
- Sebeia, N., Jabli, M., Ghith, A., Elghoul, Y., Alminderej, F.M., 2019. *Populus tremula*, *Nerium oleander* and *Pergularia tomentosa* seed fibers as sources of cellulose and lignin for the bio-sorption of methylene blue. *Int. J. Biol. Macromol.* 121, 655–665.
- Sebeia, N., Jabli, M., Ghith, A., Elghoul, Y., Alminderej, F.M., 2019. Production of cellulose from *Aegagropila Linnæi* macro-algae: chemical modification, characterization and application for the bio-sorption of cationic and anionic dyes from water. *Int. J. Biol. Macromol.* 135, 152–162.
- Simona, C., Roxana, G.Z., Grația, T.T., Violeta, P., Eugenia, E.T., Cristina, M., Anita-Laura, C., Cristian, A.N., 2020. Biopolymeric membrane enriched with chitosan and silver for metallic ions removal. *Polymers* 12 (8), 1792.
- Suhas, V.K., Gupta, P.J.M., Carrott, Randhir Singh, Monika Chaudhary, Sarita Kushwaha, 2016. Cellulose: A review as natural, modified and activated carbon adsorbent. *Bioresource Technology* 216, 1066–1076.
- Tka, N., Jabli, M., Saleh, T.A., Ghazwan, A.S., 2018. Amines modified fibers obtained from natural *Populus tremula* and their rapid biosorption of Acid Blue 25. *J. Mol. Liq.* 250, 423–432.
- Treybal, R.E., 1981. *Mass-transfer Operations*. McGraw-Hill.
- Vadivelan, V., Kumar, K.V., 2005. Equilibrium, kinetics, mechanism, and process design for the sorption of methylene blue onto rice husk. *J. Colloid Interface Sci.* 286, 90–100.
- Vijay, K.T., Stefan, I.V., 2016. Recent advances in cellulose and chitosan based membranes for water purification: a concise review. *Carbohydr. Polym.* 146, 148–165.
- Xiaoxia, L., Lu, Q., Yongzhe, D., Lifeng, H., Erwei, L., Shiming, F., Yi, Z., Tao, W., 2014. A review of recent research progress on the *Astragalus* Genus. *Molecules* 19 (11), 18850–18880.

- Younes, M., Faten, F., Elimame, E., Ridha, B.S., Mohamed, N.B., 2011. Utilisation of *Astragalus armatus* roots in papermaking. *BioResources* 6 (4), 4969–4978.
- Zakaria, B., Guillaume, P., Cédric, D., Fatima, B., Emmanuel, P., Christine, G., Philippe, M., Mohamed, D.O.E., 2015. Mediterranean semi-arid plant *Astragalus armatus* as a source of bioactive galactomannan. *Bioact. Carbohydr. Diet. Fibre* 5, 10–18.
- Zhang, X., Xiao, N., Wang, H., Liu, C., Pan, X., 2018. Preparation and characterization of regenerated cellulose film from a solution in lithium bromide molten salt hydrate. *Polymers* 10, 614.